Research Square

Preprints are preliminary reports that have not undergone peer review.
They should not be considered conclusive, used to inform clinical practice,
or referenced by the media as validated information.

Hydroclimatic Variability and Drought Characterisation in Northern Togo, 1981-2025

Malaguièhèwa Grâce Pekeyi

pekeyimphd384@st.futminna.edu.ng

Federal University of Technology (FUT Minna)

Appollonia Aimiosino Okhimamhe

Federal University of Technology (FUT Minna)

Tayo Iyanda Yahaya

Federal University of Technology (FUT Minna)

Isaiah Sule

Federal University of Technology (FUT Minna)

Research Article

Keywords: drought, standardized precipitation index (SPI), standardized precipitation-evapotranspiration index (SPEI), moisture index, water balance, northern Togo, West Africa

Posted Date: July 8th, 2026

DOI: https://doi.org/10.21203/rs.3.rs-10193491/v1

License: This work is licensed under a Creative Commons Attribution 4.0 International License.
Read Full License

Additional Declarations: No competing interests reported.

Version of Record: A version of this preprint was published at Theoretical and Applied Climatology on October 10th, 2026. See the published version at https://doi.org/10.1007/s00704-026-06621-0.

Hydroclimatic Variability and Drought Characterisation in Northern Togo, 1981-2025

Malaguièhèwa Grâce Pekeyi*[1], Appollonia Aimiosino Okhimamhe[1,2], Tayo Iyanda Yahaya[1], and Isaiah Sule[1,2]

[1]*Department of Geography, Federal University of Technology (FUT Minna), Minna, Nigeria*

[2]*West Africa Science Service Centre on Climate Change and Adapted Land Use (Climate Change and Human Habitat), Federal University of Technology (FUT Minna), Minna, Nigeria*

Corresponding author: Malaguièhèwa Grâce Pekeyi

Email: pekeyimphd384@st.futminna.edu.ng

ABSTRACT

Climate change is increasingly intensifying drought conditions across West Africa, with northern Togo emerging as one of the most drought-vulnerable sub-regions of the continent yet lacking locally adapted tools for effective droughts monitoring and moisture deficit assessment. This study analyses rainfall variability, drought frequency and moisture deficit across three agroecological zones of northern Togo from 1981 to 2025. Three synoptic stations were combined with NASA Prediction of Worldwide Energy Resources reanalysis and Climate Hazards Group InfraRed Precipitation with Stations satellite data. The Hamed-Rao modified Mann-Kendall test, Sen slope estimator and three change-point tests (Pettitt, Buishand, and Standard Normal Homogeneity Test) were applied to annual, seasonal and monthly timescales. The Standardized Precipitation Index, Standardized Precipitation-Evapotranspiration Index and Willmott-Feddema Moisture Index were calculated to evaluate drought conditions and moisture availability. No statistically significant precipitation trends were detected at any station, while a significant warming of +0.27 to +0.34 °C per decade amplified evapotranspiration demand. Consequently, the two drought indices have progressively diverged since 2003, a signal invisible when considering only precipitation, driven by a spatially coherent temperature change point identified around 2001-2003. All stations recorded exclusively negative Moisture Index values, confirming a permanent deficit of water in the entire area. Spatial analysis revealed predominantly positive moisture trends, with significant negative trends confined to fewer than 8% of grid cells. These findings emphasize the need for temperature-sensitive drought indices in early warning systems and provide critical insights for rain-fed cereal production and water resource management in one of West Africa's most climate-exposed regions.

Keywords: drought, standardized precipitation index (SPI), standardized precipitation-evapotranspiration index (SPEI), moisture index, water balance, northern Togo, West Africa.

1 Introduction

Climate change is one of the most urgent environmental issues facing the 21st century and has a profound impact on the global water cycle. This is evident in changing rainfall patterns, increased evapotranspiration demand, and more frequent extreme weather and hydrological event (Cosgrove et al. 2000;Calvin et al. 2023,Wang and Liu 2023). This is one of the region's most vulnerable to climate change. According to the IPCC (2023), an increase in temperature of 1.5°C or more compared to pre-industrial levels would cause irreparable damage to water reserves and agricultural productivity. Drought can be classified as meteorological, agricultural, hydrological or socio-economic (Wilhite and Glantz 1985; Mishra and Singh 2010),), an increase in temperature of more than 1.5 °C compared to pre-industrial levels would cause irreversible damage to water resources and agricultural productivity. Drought can be classified as meteorological, agricultural, hydrological or socio-economic (Vicente-Serrano et al. 2010; Beguería et al. 2014).

In sub-Saharan Africa, a terrible drought occurred in the 1970s and 1980s, followed by a spatially heterogeneous rainfall recovery from the 1990s onwards (Barbé et al. 2002; Lebel and Ali 2009; Rauch et al. 2025). Recent analyses confirm persistent precipitation deficits in northwestern Africa, where a SPI-SPEI divergence caused by climate change increases the risk of drought regardless of precipitation trends (Akinwale T. Ogunrinde et al. 2024), (Tefera et al. 2024; Mohammed et al. 2024; Bodjrènou et al. 2025).

Northern Togo, which extends through the savannah and transition zones towards the Sahel, is particularly vulnerable to variations in rainfall and water scarcity in agriculture. However, Togolese hydrological literature is quite scarce compared to that of neighbouring countries such as Nigeria (Ogunrinde et al., 2019), Ghana (Nkrumah et al., 2014) and Burkina Faso (Tazen et al., 2019). Current research on Togo documents an increase in reference evapotranspiration and aridity (Djaman and Ganyo, 2015), a decrease in precipitation at 80% of meteorological stations between 1961 and 2001 (Djaman, 2017), the predominance of drought periods based on the SPI index in southern stations (Koudahe et al., 2017), a shortening of the rainy season in northern regions since the 1970s (Djaman, 2017), and spatial variability in precipitation and temperature trends in the savannah region (Yao et al., 2023).

Northern Togo, spanning the Sudanian savanna and sub-Sahelian transition zones, is particularly vulnerable to variations in rainfall and water scarcity in agriculture. However, Togolese hydrological literature is quite scarce compared to that of neighbouring countries such

as Nigeria (Ogunrinde et al. 2019), Ghana (Nkrumah et al. 2014), and Burkina Faso (Tazen et al. 2019). Current research on Togo documents an increase in reference evapotranspiration and aridity (Djaman and Ganyo 2015),), a decrease in precipitation at 80% of meteorological stations between 1961 and 2001(Djaman 2017), the predominance of drought periods based on the SPI index in southern stations (Koudahe et al. 2017), a shortening of the rainy season in northern regions since the 1970s (Djaman 2017), and spatial variability in precipitation and temperature trends in the savannah region (Yao et al. 2023). More recently, extreme precipitation events in the Oti river basin in northern Togo have been analysed using climate indices and CORDEX-Africa projections for the period between 1961 and 2022. This analysis has revealed significant trends related to extreme precipitation linked to the West African monsoon and interannual variability induced by the El Niño-Southern Oscillation (ENSO) phenomenon. Despite these advances, critical gaps remain. Firstly, all analyses conducted in Togo are based on sparse station networks, without spatial extension through reanalysis or satellite products. This limits their spatial representativeness. Bodjrènou et al. (2025) identified this limitation in neighbouring Benin. The authors have demonstrated that studies based on one or three stations per climatic zone do not adequately capture the variability of droughts at a subregional level. They have also demonstrated that reanalysis data sets offer a promising alternative to address these gaps. Secondly, there is no evidence that research has been conducted applying the Willmott-Feddema moisture index (MI) to characterise the permanent water deficit regime in the three agro-ecological zones of northern Togo, or to quantify the geographical covariates (latitude, altitude and mean potential evapotranspiration (PET)) that regulate the north-south water deficit gradient. Third, Ogunrinde et al. (2024) have demonstrated that the variability of drought at different scales in West Africa is due to complex interactions between large-scale climate indices and regional moisture dynamics, with the Sahel experiencing the most severe and prolonged drought trends. However, there is no evidence of an equivalent analysis that integrates SPI, SPEI and MI with a mapping of spatial trends for northern Togo. Furthermore, the recent intensification of drought risk due to the divergence of SPI-SPEI induced by warming, documented by Tefera et al. (2024), in Ghana and Burkina Faso, and confirmed for 2023 by an analysis (Kongo and Arreyndip 2025) showing how warming induced by El Niño has amplified the drought independently of precipitation anomalies in the Sahel, has not been evaluated for northern Togo based on a period of observation extending to 2025. There is also no information on previous studies that have simultaneously integrated

seasonal observations with gridded reanalysis products over the entire area of the three agroecological zones in northern Togo, or that have systematically quantified the geographical covariates that regulate the spatial gradient of moisture deficit in the region.

This research has addressed these deficiencies with three objectives: (i) evaluate precipitation and temperature trends using several complementary statistical methods; (ii) characterise the frequency, severity and duration of drought using the Standardised Precipitation Index (SPI), the Standardised Precipitation-Evapotranspiration Index (SPEI) and the Standardised Moisture Index (MI); and (iii) map spatial moisture deficit trends using NASA POWER and CHIRPS and quantify their geographical variables using Spearman's correlation. The peculiarity of this study lies in the simultaneous application of the soil moisture index (MI), the standardized precipitation index (SPI) and the standardized precipitation-evapotranspiration index (SPEI). The results of this study are complemented by comprehensive mapping of spatial trends at two resolutions (0.5° and 0.05°) and the application of three testing procedures for identifying inflection points, including the modified Hamed-Rao Mann-Kendall test, and a study period (1981-2025) extending four to ten years beyond that of most comparable regional analyses.

2 Materials and Methods

2.1 Study area

Northern Togo is located between latitudes 8.5°N-11.2°N and longitudes 0.3°E-1.5°E on the western coast of Africa. It is bounded by Burkina Faso to the north, Ghana to the west, and Benin to the east (Fig. 1). The climate in this region is regulated by the western African monsoon and the seasonal migration of the intertropical convergence zone (Nicholson 2013; Biasutti 2019). Precipitation is unimodal (from May to October), with mean annual rainfall decreasing from 1260 mm in Sokodé (8.98° N) to 1050 mm in Mango (10.37° N) (Djaman 2017; Yao et al. 2023). Average temperatures range from 22 °C to 38 °C, peaking during the Harmattan period (November to April). Three synoptic stations have been selected (see Table 1): Sokodé (Tall Grass Savanna, TGS), Kara (Short Grass Savanna, SGS) and Mango (Marginal Savanna, MS). These correspond to the three agro-ecological zones defined by Djaman (2017) and Ali (2021). Altitudes range from 143 to 423 m above sea level (Copernicus DEM 2021), and the Atacora mountain range (600 m) forms the western watershed.

Table 1 Meteorological stations used in this study.

Station	Latitude (°N)	Longitude (°E)	Elevation (m)	Agro-eco. zone	Period
Sokodé	8.98	1.14	371	Tall Grass Savanna	1981-2025
Kara	9.55	1.19	423	Short Grass Savanna	1981-2025
Mango	10.37	0.47	143	Marginal Savanna	1981-2025

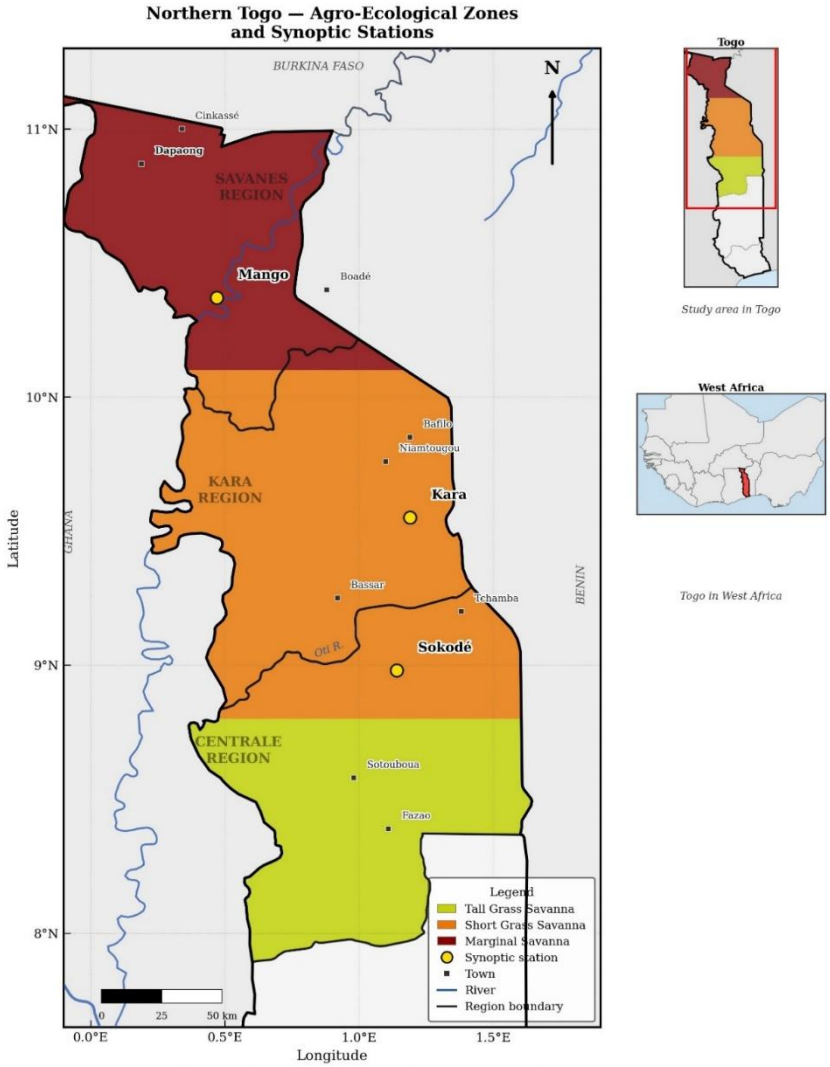


Fig. 1 Northern Togo showing the three study regions (Centrale, Kara, Savanes), agro-ecological zones (adapted from FAO/IIASA Global AEZ database, 2021), hydrography, major towns, and the three synoptic stations (yellow circles) used in this study. Insets show the study-area location within Togo (top) and West Africa (bottom).

2.2 Data collection and analysis

The database includes monthly precipitation series, as well as maximum (T_(max)), mean (T_(mean)) and minimum (T_(min)) temperature series. These were obtained from data provided by the National Meteorological Service of Togo (DGMN) between 1981 and 2025. The data quality was evaluated using the double-curve mass technique (Kohler 1949); homogeneity was evaluated using the point change test described in Section 2.5; and missing monthly values were evaluated using the normal relationship methodology. The NASA POWER project (Zhang et al. 2010) provided monthly climatological data with a resolution of 0.5° for the period from 1981 to 2024 (84 grid points). The ERA5-Land model was considered but ultimately rejected due to inadequately parametrized Saharan convective systems at mesoscale (Sylla et al. 2013), as well as an artificial increase in Saharan precipitation after the mid-1990s (Hersbach et al. 2020). To analyse trends in pixels between 1981 and 2024, we used CHIRPS v2.0 (Funk et al. 2015) with a resolution of 0.05°. Validation using meteorological station observations (Table 2) revealed a moderate temporal correlation (r = 0.43-0.57) and a systematic biases (Mango: +19.7%). For this reason, the maps should be interpreted as showing relative trends rather than absolute values. The analysis of stationary series (precipitation, SPI, SPEI, MI, inflection point test and period analysis) covers the entire period from 1981 to 2025. Conversely, the spatial analysis using NASA POWER and CHIRPS products was limited to the period from 1981 to 2024, since these mosaic products were only available from December 2024 when the analysis was conducted. The two-year difference did not affect the main conclusions, as the temperature change (2001-2003) and divergence between the SPI and SPEI indices after 2003 are robust characteristics of the 1981-2024 period. These were confirmed independently by station data and analytics.

Table 2 Validation of NASA POWER annual precipitation against station observations (1981-2024, n = 44).

Station	Obs. mean (mm yr^{-1})	POWER mean (mm yr^{-1})	Bias (%)	r	NSE
Sokodé	1262	1254	−0.6	0.43	−0.14
Kara	1276	1158	−9.3	0.47	−0.32
Mango	1058	1267	+19.7	0.57	−1.87

2.2.1 Drought and water balance indices

The annual ETp estimation was performed using temperature as the independent variable, according to the methodology developed by Hargreaves-Samani (1985) and adapted for areas without irradiance, humidity and wind speed data (Droogers and Allen 2002; Djaman 2017):

$$PET = 0.0023 \times Ra \times \sqrt{(Tmax - Tmin)} \times (Tmean + 17.8) \times d \quad (1)$$

Where Ra represents extraterrestrial solar radiation (mm/day^{-1}) (Allan et al. 1998), $T_(max)$, $T_(min)$ and $T_(mean)$ are the monthly mean temperatures (°C) and d is the number of days in the month. The Hargreaves and Samani methodology was applied and validated in previous hydroclimatic studies in Togo (Djaman and Ganyo 2015; Djaman 2017). However, it should be recognised that the Hargreaves and Samani methodology may underestimate PET in strong wind conditions and overestimate it in very humid environments, due to its exclusive dependence on temperature as a proxy for net radiation (Droogers and Allen 2002). In northern Togo, where the harmattan generates violent winds and low humidity, this methodology may slightly underestimate the PET of the dry season, which would reduce the SPEI and MI deficits calculated. This limitation is intrinsic to environments with limited data and does not affect the direction of the trends presented, since any systematic error in estimating the PET would remain constant throughout the study period.

The Willmott-Feddema, (1992) Moisture Index (MI) (Eq. 2) quantifies the annual water balance on a scale from -100 (extreme aridity) to +100 (maximum humidity); (Mccabe and Wolock 2007; Ogunrinde et al. 2019):

$$MI = 100\left(\frac{P}{PET} - 1\right) if\ P < PET; \quad MI = 100\left(1 - \frac{PET}{P}\right) if\ P \geq PET \quad (2)$$

P stands for the annual rainfall (in mm). The reference value of the MI index = -20 marks the boundary between semi-arid and subhumid regions (Willmott and Feddema 1992). The SPI index (McKee et al. 1993) was calculated over a period of 12 months and a two-parameter gamma distribution was fitted to the annual rainfall, whereby the density function $H(x) = q + (1 -$

$q)G(x)$ was transformed into a standard normal distribution (Abramowitz and Stegun 1965). The reference values for classifying the SPI index follow those of McKee et al. (1993): 'moderate dryness' for an SPI index below -1, 'very dry' for an SPI index below -1.5, and 'extremely dry' for an SPI index below -2. The SPEI (Vicente-Serrano et al. 2010) builds on the SPI by replacing the precipitation with the monthly water balance $Di = Pi - PETi$, applying a Pearson-III distribution to *Di* and performing an inverse normal transformation. The inclusion of PET makes the SPEI more sensitive to the intensification of droughts due to climate change than the SPI (Beguería et al. 2014; Spinoni et al. 2019). All indices were calculated for the three seasons (1981-2025) and for the 84 points of the NASA-POWER-Mesh (1981-2024).

2.2.2 Trend analysis

The non-parametric Mann-Kendall (MK) test (Mann 1945; Kendall 1975) was used as the primary method for detecting trends, since it does not require any distributional assumptions and is robust to outliers (Gocic and Trajkovic 2013; Ogunrinde et al. 2019). The S test statistic and the variance $\sigma^2(S)$ follow standard formulations (Mann 1945), and the corresponding significance values are $p \leq 0.05\ (|Z| \geq 1.96), p \leq 0.01\ (|Z| \geq 2.576), p \leq 0.001\ (|Z| \geq 3.291)$. When significant first-order autocorrelation is detected ($|r_1| > 2/\sqrt{n} \approx 0.30\ for\ n = 44$), the MK-HR test of Hamed and Ramachandra Rao (1998) corrects the S variance to account for the effective sample size, n/n*. The standard MK and MK-HR tests were applied using the *pyMannKendall* package (Hussain and Mahmud 2019). The trend magnitude was estimated using Sen (1968) slope estimator (Eq. 3):

$$\beta = median[(x_j - x_i)/(j - i)],\ 1 \leq i < j \leq n \quad (3)$$

Precipitation and MI are expressed in mm/year, while temperatures are indicated in °C/decade. To isolate the long-term variability of precipitation, a five-point Hanning filter (von Storch 1995) was applied, and the annual precipitation variability index, $\delta i = (Pi - \mu)/\sigma$ (Gocic and Trajkovic 2013), was used to classify abnormal years.

2.2.3 Homogeneity and change-point detection

Three complementary non-parametric tests were applied to detect changes in trends in annual precipitation and temperature series. The Pettitt test (1979) identifies a unique turning point in year τ by maximising the absolute value of the sum of the signs of the deviations between the observations and the mean (i.e. $|U_{tj}| = |\Sigma\Sigma\, sgn(X_i - X_j)|$). The Buishand test (1982) detects a trend change through the adjusted partial sums, $S * k = (1/\sigma)\Sigma(X_i - \bar{X})$, and the SNHT test (Alexandersson 1986) maximises $T_0 = [\tau\bar{z}^2{}_1 + (n - \tau)\bar{z}^2{}_2]$ in the candidate crops. Using several of these tests is recommended because convergence of the results provides stronger evidence of a true structural transformation than any individual test (Pettitt 1979; Buishand 1982). All of these tests were implemented using the pyhomogeneity package (Hussain and Mahmud 2019).

2.2.4 Spatial analysis and covariates

The MK test and the Sen index were applied independently to the annual time series of the meteorological drought index (MI), the precipitation drought index (SPI) and the precipitation-evapotranspiration drought index (SPEI), for each of the 84 NASA-POWER grid points, as well as for each CHIRPS pixel. In Sen's slope maps, significant cells ($p \leq 0.05$) were retained and insignificant ones hidden. NASA-POWER values were interpolated using bilinear interpolation and the means were then calculated using the Gauss methodology ($\sigma = 0.9$ grid cell). Spearman's rank correlation coefficient (ρ_s) was calculated for the following variables at the 84 grid points: length, latitude, altitude, mean deficit of precipitation (MI), mean potential deficit of precipitation (PET) and mean deficit of precipitation (P), as well as Sen's slopes (CMI, CSPI and CSPEI), in order to identify the main spatial factors determining the deficit of precipitation (Gocic and Trajkovic 2013). All operations were executed in Python 3.12 using NumPy 1.26, SciPy 1.12, Pandas 2.2, Matplotlib 3.8, pyMannKendall 1.4.3 and pyHomogeneity 1.0.0.

3 Results and Discussion

3.1 Precipitation, temperature climatology, and trend analysis

Mean annual precipitation decreases northward: Sokodé (1257 mm) > Kara (1268 mm) > Mango (1051 mm); (Table 3). The slightly higher rainfall at Kara relative to Sokodé, despite its more northerly position, reflects orographic enhancement by the Atacora mountain chain (600 m), which promotes convective uplift during the monsoon season (Djaman 2017). Coefficients of variation (CV) of 12.5-15.2% indicate that in approximately one year out of five, annual rainfall deviates by more than 190 mm from the mean, generating recurrent crop stress even outside formal drought years (Gadedjisso-Tossou et al. 2021). Annual mean temperatures increase northward (Sokodé: 27.2°C, Kara: 28.3°C, Mango: 29.8°C), creating the aridity gradient documented by the MI (Section 3.3). Lag-1 serial correlations for annual precipitation range from -0.18 to +0.18 (all within the 95% bounds of ±0.30), validating the application of the standard MK test without pre-whitening.

Table 3 Descriptive statistics of annual precipitation (1981-2025) and Mann-Kendall trend test results. MK-HR: Hamed-Rao modified test. *** p < 0.001; ns = not significant.

Station	Mean (mm)	CV (%)	MK Z	MK-HR Z	p-value	Sen slope	Sig.
Sokodé	1257	12.5	0.53	0.53	0.599	+1.07 mm yr^{-1}	ns
Kara	1268	15.2	0.14	0.14	0.887	+0.32 mm yr^{-1}	ns
Mango	1051	15.0	0.80	0.80	0.424	+1.19 mm yr^{-1}	ns
Sokodé (temp.)	27.2°C		5.43	5.43	<0.001	+0.27°C dec^{-1}	***
Kara (temp.)	28.3°C		4.14	4.14	<0.001	+0.34°C dec^{-1}	***
Mango (temp.)	29.8°C		4.79	4.79	<0.001	+0.28°C dec^{-1}	***

No significant annual precipitation trends were detected at any station (p > 0.40), which is consistent with the results of similar monitoring networks in West Africa, such as in Filtered precipitation series according to Hanning (Fig. 2) show a significant drought phase between 1982 and 1988, followed by a partial recovery from 1993 onwards. This trend is consistent with the

resumption of rainfall observed in the Sahel, attributed to the modification of the AMO phase and the decrease in Saharan dust concentration (Biasutti 2019; Rauch et al. 2025). Although the positive slopes are not significant (ranging from +0.32 to +1.19 mm per year), they are consistent with the partial Sahelian recovery, but do not differ significantly from zero statistically. This result is consistent with that of Tefera et al. (2024), who did not identify a significant annual trend in Sudan and other West African countries such as Ghana and Burkina Faso. However, annual mean temperatures show a highly significant upward trend in the three regions (see Table 3; $p < 0.001$ for all three regions), with a warming rate ranging from 0.27 to 0.34 °C per decade. These values exceed the global average (IPCC, 2021) and are consistent with the acceleration of warming in the Soudano-Sahelian region (Sylla et al. 2013; Yaméogo 2024). Regarding seasonality, significant positive trends in precipitation were detected in October in Mango ($Z = 2.22$, $p = 0.026$) and Sokodé ($Z = 2.02$, $p = 0.043$), which corroborates the strengthening of the Intertropical Convergence Zone (ITCZ) during its final phase, as reported by Panthou et al. (2018).

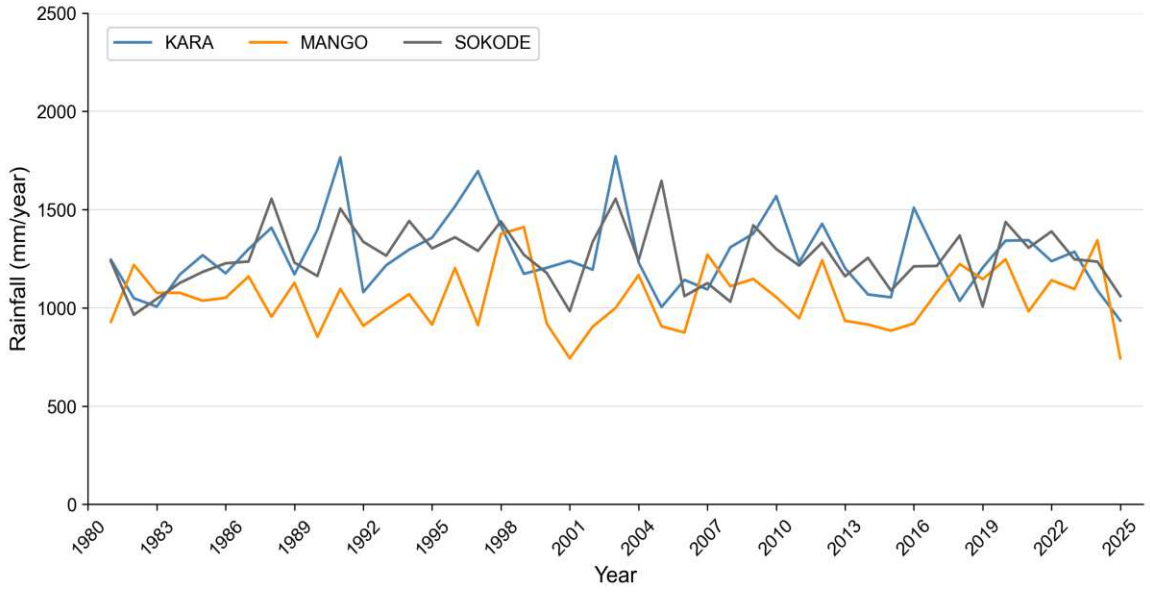


Fig. 2 Annual precipitation time series at the three synoptic stations.

3.2 Change-point detection in precipitation and temperature

The Petit test revealed no statistically significant variations in precipitation at the measurement stations (all p-values were greater than 0.05), a result that aligns with the non-significant MK data

presented in Table 4. The observed alteration in Sokodé (1987/1988, K = 140) coincided with the end of the Sahelian drought phase (132.3 mm, +11.5%), but this was not statistically confirmed. Recent transition phases observed in Karakol (CP = 2012/13) and Mango (CP = 2016/17) suggest potential variation in northern stations, which is consistent with the trend of Sahelian reactivation expanding from north to south (Lebel and Ali 2009; Rauch et al. 2025). However, additional data are needed to confirm this trend. Conversely, the Pettit test revealed consistent and statistically significant alterations ($p < 0.001$) throughout the year. Between 2001 and 2002, Sokodé registered an increase of 0.594 °C (2.23%), Kara an increase of 0.852 °C (3.13%), and Mango an increase of 0.653 °C (2.27%) (Table 4). The Buishand and SNHT tests confirm these variations. From a physical standpoint, the sudden heatwaves of 2001 and 2003 corresponded to the Atlantic Multidecadal Oscillation (AMO) transitioning to a positive phase. This event caused an increase in the intensity of warming in the Sahel and altered the major atmospheric currents (Biasutti 2019; Sylla et al. 2013), occurring after the La Niña cooling episode between 1998 and 2001 (IPCC 2021). Between 1998 and 2001, the La Niña phenomenon cooled the region (IPCC, 2021), which explains the differences between the SPI and SPEI indices in Fig. 3.

Table 4 Pettitt change-point test results for annual precipitation and mean temperature at the three synoptic stations of Northern Togo (1981-2025).

Station	Variable	CP year	K	p-value	Sig.	μ_1	μ_2	Δ
Sokodé	Precip. (mm yr^{-1})	1987/1988	140	0.566	n.s.	1145.4	1277.7	+132.3 (+11.5%)
Kara	Precip. (mm yr^{-1})	2012/2013	106	0.970	n.s.	1296.7	1198.0	−98.7 (−7.6%)
Mango	Precip. (mm yr^{-1})	2016/2017	110	0.917	n.s.	1036.0	1111.0	+74.9 (+7.2%)
Sokodé	Temp. (°C)	2001/2002	400	<0.001	***	26.695	27.289	+0.594 (+2.23%)
Kara	Temp. (°C)	2002/2003	436	<0.001	***	27.202	28.054	+0.852 (+3.13%)
Mango	Temp. (°C)	2002/2003	392	<0.001	***	28.792	29.445	+0.653 (+2.27%)

*n.s.: not significant ($p > 0.05$). ***: $p < 0.001$. μ_1: mean before CP; μ_2: mean after CP.*

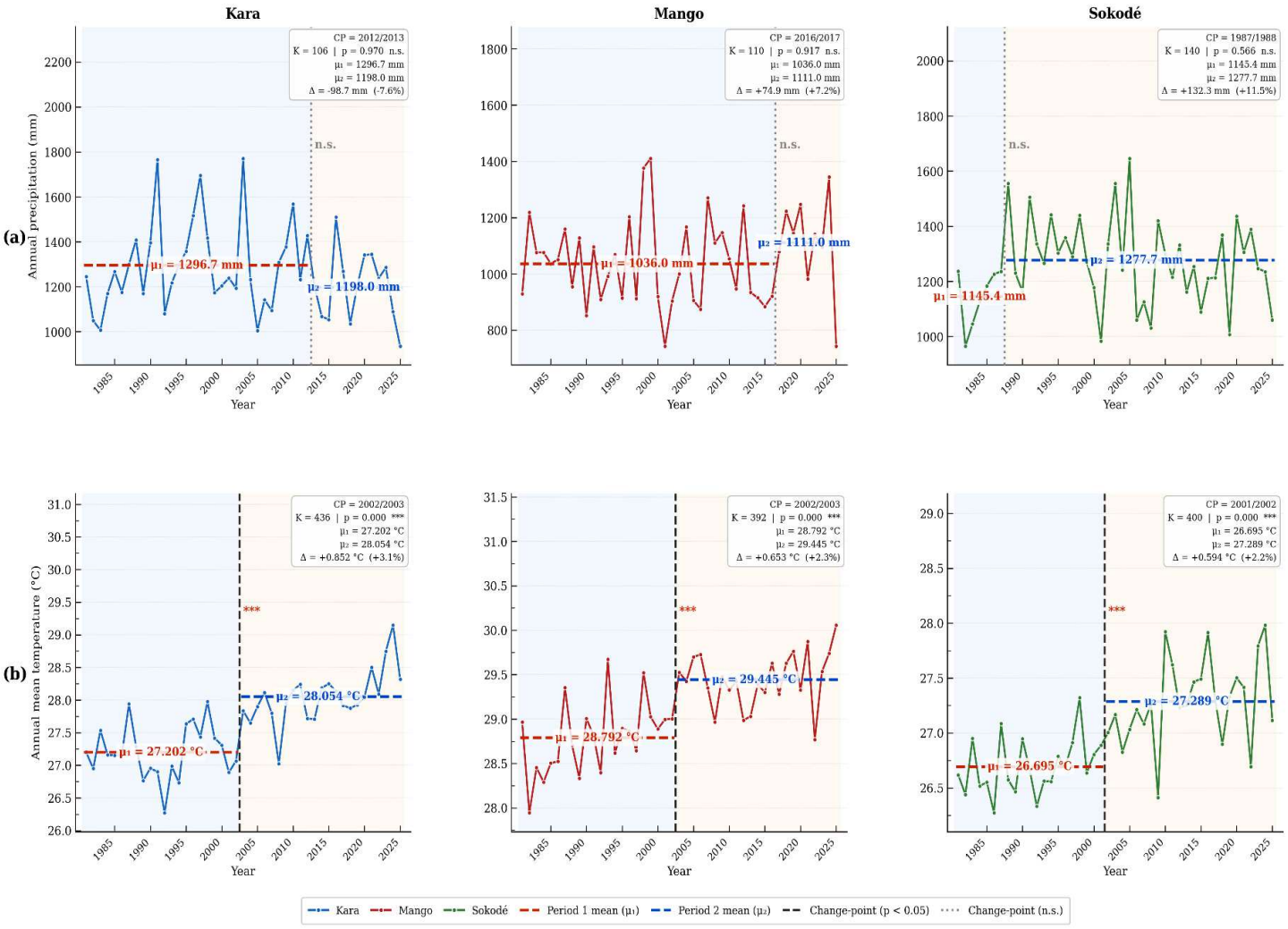


Fig. 3 Change-point analysis of annual precipitation (a) and annual mean temperature (b) at the three synoptic stations of Northern Togo (1981-2025). Vertical dotted line (a): most probable but non-significant Pettitt CP. Vertical dashed line (b): statistically significant Pettitt CP ($p < 0.001$). Red dashed: mean before CP (μ_1); blue dashed: mean after CP (μ_2).

3.3 Drought characterisation: SPI, SPEI, and temperature-driven intensification

All three stations recorded periods of drought (Table 5). The most intense phenomenon observed in Mango occurred in 2025 (SPI = -2.16, classifying it as extreme drought), while the most intense phenomenon observed in Sokodé occurred in 1982 (SPI = -2.02, also classifying it as extreme drought). In contrast, 2025 in Kara was characterised by significant drought (SPI = -1.94), which is not yet classified as extreme. The persistence of extreme drought until 2025, despite

precipitation resuming after 1990, indicates that the risk of drought in northern Togo has not decreased. The SPI trend for the three locations is positive but not significant ($Z = 0.42$-0.87, $p > 0.38$), a result consistent with the findings of Ababio et al. (2024) and Ogunrinde et al. (2024). However, the absence of a significant SPI trend does not necessarily imply a reduction in risk. In the context of global climate change, the actual risk of drought, as measured by the SPEI index, can increase even in the absence of a trend in precipitation (Vicente-Serrano et al. 2010). Since 2003, the stations have recorded SPEI values lower than SPI values (figures 4 and 5). This situation is directly related to the increase in temperatures observed since 2002 (Section 3.2), which has increased the potential evapotranspiration (PET) and caused a water deficit. Tefera et al. (2024) confirmed this discrepancy between the SPI and SPEI indices in a region similar to Ghana and Burkina Faso. To confirm this statistical difference, a Mann-Whitney U test adapted for comparing two independent sub-periods of unequal lengths was used for the annual SPI-SPEI values in each station (Table 6). This test was applied to the period before 2003 (1981-2002, $n = 22$) and the period after 2003 (2003-2025, $n = 23$). The median difference (SPI-SPEI) shifted from negative to positive at all three sites: Sokodé (from -0.07 to +0.11), Kara (from -0.03 to +0.11) and Mango (from -0.12 to +0.11). This change was statistically significant in Sokodé ($U = 158$, $p = 0.032$), but not in Kara ($U = 179$, $p = 0.095$) or Mango ($U = 196$, $p = 0.199$). These results suggest that the divergence between the SPI and SPEI in Sokodé after 2003 is statistically significant. In Kara and Mango, the same trend is observed, but remains within the limits of natural interannual variability.

Table 5 Drought characteristics at the annual SPI-12 scale (1981-2025). Classes: McKee *et al.* (1993).

Station	Min SPI	Year	Moderate (−1.5<SPI≤−1.0)	Very dry (−2.0<SPI≤−1.5)	Severe (SPI≤−2.0)	Total
Sokodé	−2.02	1982	4	3	1	8
Kara	−1.94	2025	7	1	0	8
Mango	−2.16	2025	3	0	2	5

Table 6 Mann-Whitney U test comparing the distribution of annual (SPI - SPEI) differences between the pre-2003 (1981-2002) and post-2003 (2003-2025) sub-periods at each station. Bold p-value indicates significance at α = 0.05.

Station	n (pré / post-2003)	Médiane (SPI-SPEI) pré-2003	Médiane (SPI-SPEI) post-2003	Mann-Whitney U	p
Sokodé	22 / 23	−0.07	+0.11	158	0.032
Kara	22 / 23	−0.03	+0.11	179	0.095
Mango	22 / 23	−0.12	+0.11	196	0.199

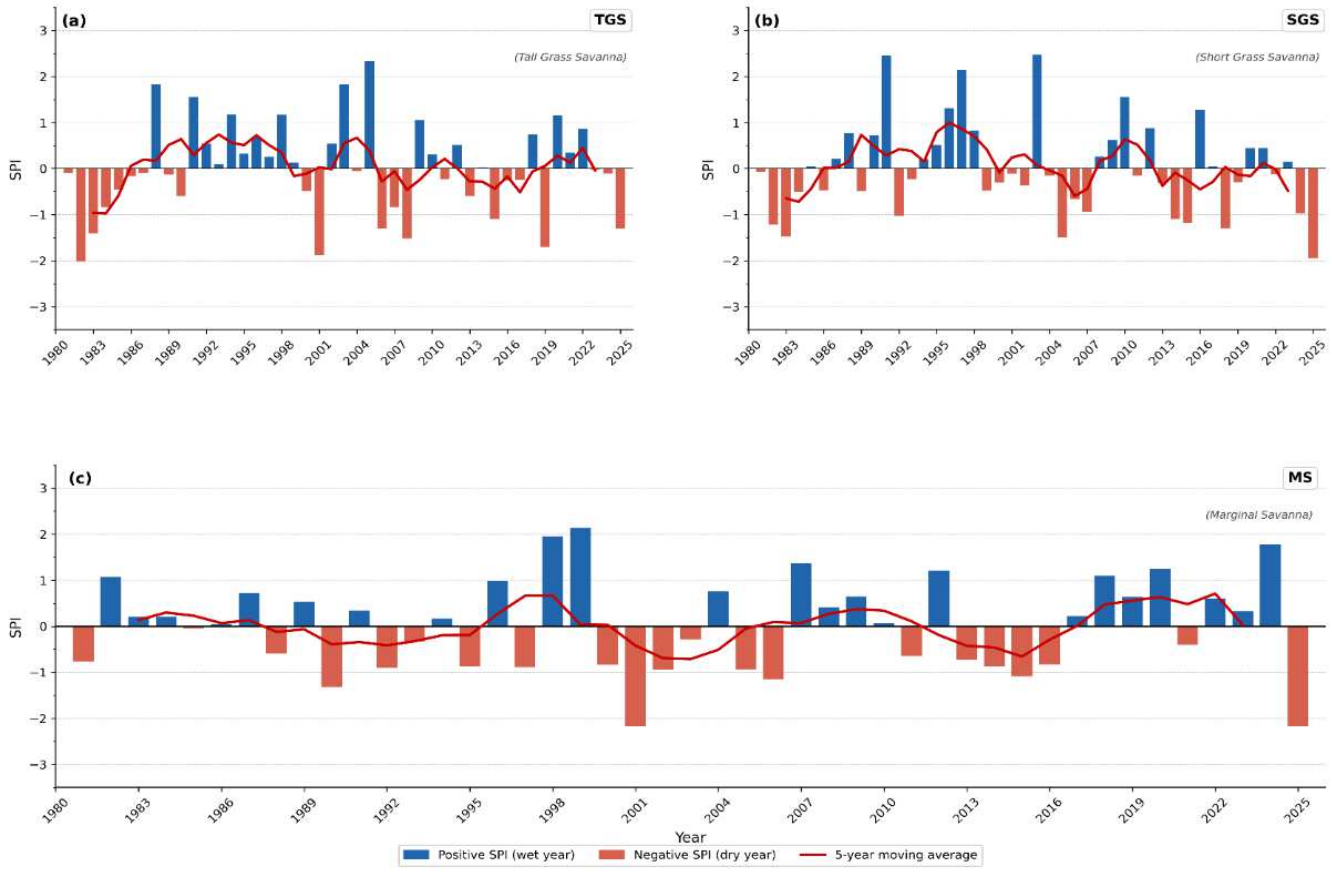
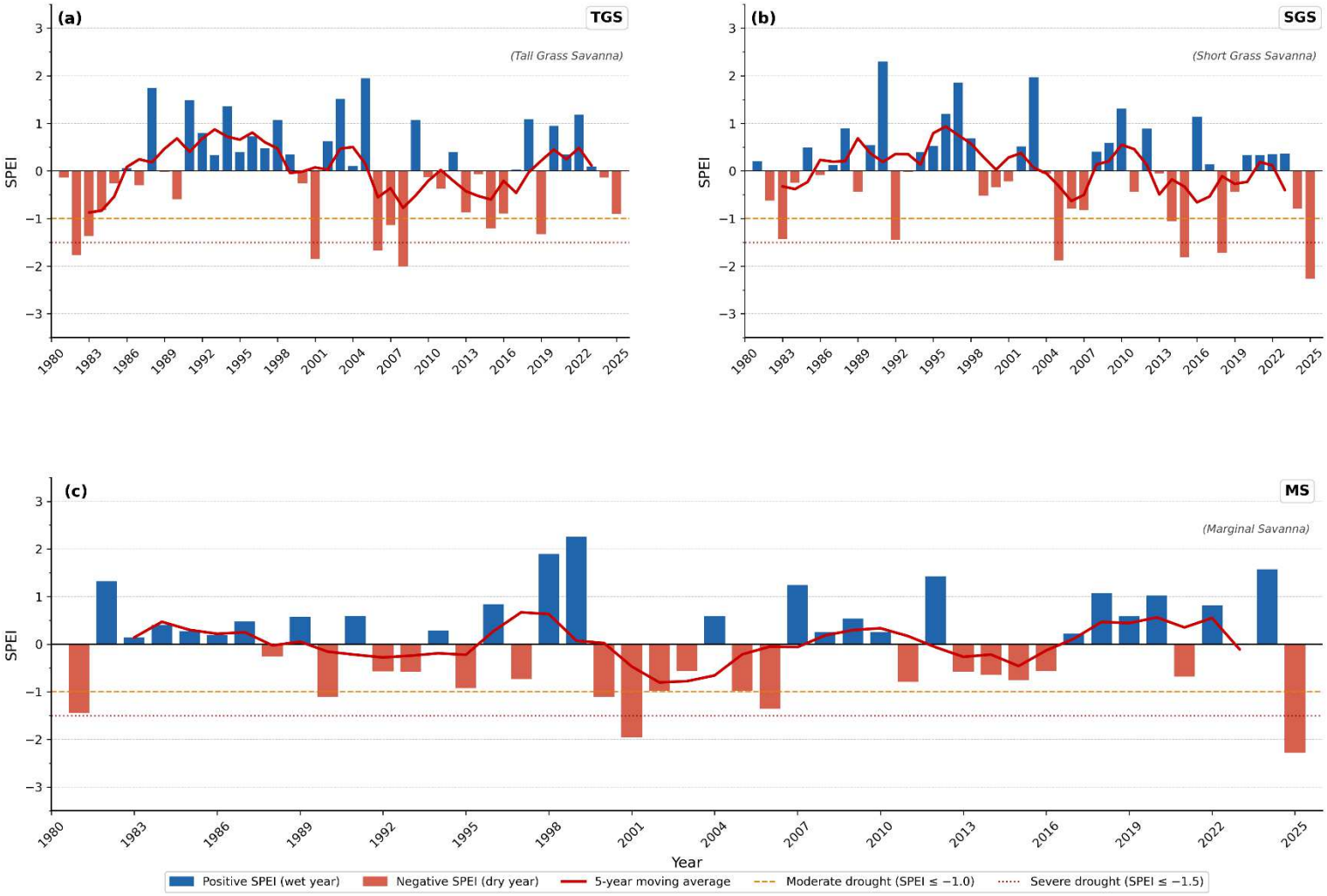


Fig. 4 Annual SPI-12 time series and 5-year centred moving average (red line) at the three agro-ecological zones of Northern Togo (1981-2025). TGS: Tall Grass Savanna (Sokodé); SGS: Short Grass Savanna (Kara); MS: Marginal Savanna (Mango).



369

370 **Fig. 5** Annual SPEI-12 time series and 5-year centred moving average at the three agro-ecological
371 zones of Northern Togo (1981-2025). TGS: Tall Grass Savanna (Sokodé); SGS: Short Grass
372 Savanna (Kara); MS: Marginal Savanna (Mango).

373 **3.4 Moisture deficit: spatial pattern and sub-period warming dynamics**

374 Throughout the study period, all cells in the NASA-POWER grid and the three stations recorded
375 exclusively negative MI values, confirming a permanent water deficit in the entire area (Fig. 6 and
376 7, as well as tables 6 and 7). Values of the Normalised Difference Vegetation Index (NDVI) varied
377 between -20 in the southern central plains and -60 in the northern savannahs, reflecting the aridity
378 gradient from north to south. This trend was confirmed by Spearman's correlation coefficients.
379 Latitude (ρs = -0.850 with MI, $p < 0.01$) and mean temperature of evapotranspiration (PET) (ρs =

-0.903, p <0.01) were the most significant spatial factors, while precipitation played a less significant, though still relevant, role (ρs = +0.757, p <0.01). Values of MI below -20 (the limit of the semi-arid zone) were recorded in all seasons and years, indicating that subsistence agriculture remains below the water security threshold. Notably, the maximum vegetation index value (MI = -2.9) in Kara indicates that savanna with limited herbaceous coverage can reach hydric equilibrium in the event of exceptionally abundant monsoon rains. This situation is consistent with the influence of the Atacora mountain chain. Interannual variability of the CMI is greater in Kara (30.0%) than in Mango (17.0%), reflecting greater variability in the hydrological regime in the central area where there is a transition between subhumid and semi-arid zones. In Mango, the hydrological regime remains arid regardless of annual variations in precipitation. The curves of the CMI, CSPI and CSPEI values demonstrate a strong correlation (r = 0.94-0.99, p < 0.01), confirming that the three indices respond to the same large-scale hydrological dynamics

Table 7 Moisture Index (MI) statistics by agro-ecological zone (1981-2025) and key Spearman rank correlations among spatial variables (84 NASA POWER grid points, 1981-2024). ** p ≤ 0.01.

Zone / Variable	Station	Mean MI	CV (%)	Spearman ρs with MI	p-value
Tall Grass Savanna	Sokodé	−32.1	28.1	—	—
Short Grass Savanna	Kara	−34.2	30.0	—	—
Marginal Savanna	Mango	−47.2	17.0	—	—
Latitude	—	—	—	−0.865	<0.01**
Mean PET	—	—	—	−0.929	<0.01**
Mean P	—	—	—	+0.757	<0.01**

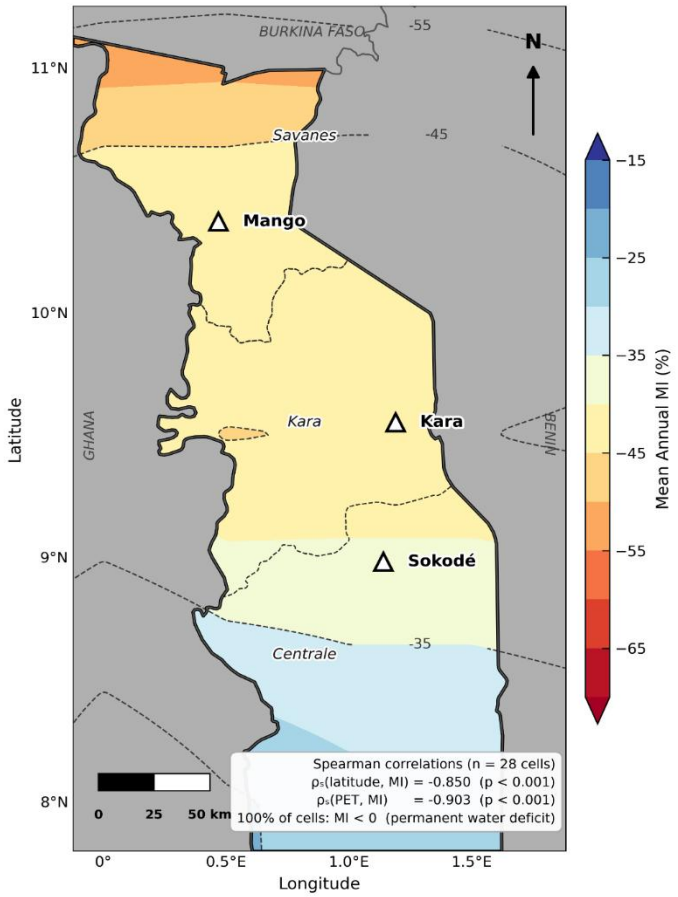


Fig. 6 Spatial distribution of mean annual Moisture Index (MI, %) over Northern Togo (NASA POWER reanalysis, 1981-2024, 0.5° grid). Grey shading: neighbouring countries. Triangular markers: synoptic stations. All grid cells record negative MI, confirming a permanent water-deficit regime. The south-to-north aridity gradient is driven by latitude ($\rho s = -0.850$, $p < 0.01$) and mean PET ($\rho s = -0.903$, $p < 0.01$).

The analysis by subperiod (Table 8) reveals a spatially heterogeneous warming pattern. During the 12-year drought recovery period (1981-1992), Sokodé experienced a significant increase in precipitation (+31.50 mm per year, $p = 0.047$). No other significant precipitation trends were observed, confirming the stalling of the recovery after 1992. In terms of temperature, Kara experienced a concentrated increase beginning in 2002 (0.333 °C per decade, $p = 0.003$), which confirms the abrupt variation in Pettitt's test. Mango showed a significant temperature increase before 2002 (+0.308 °C per decade, $p = 0.011$), suggesting that the transition to higher temperatures at this northernmost station began earlier. Sokodé showed a continuous increase in temperature in both periods (+0.186 and +0.216 °C per decade, Figure 7). Despite the

heterogeneity among the stations, the constant trend of increasing temperature in all of them in all periods explains the progressive divergence between the SPI and SPEI indices after 2003(Bodjrènou et al. 2025; Tefera et al. 2024).

Table 8 Sub-period Mann-Kendall trend analysis for annual precipitation and mean temperature at Northern Togo stations.

Station	Variable	Period	n	Sen's slope	p-value	Sig.
Precipitation (mm yr⁻¹)						
Sokodé	Precip. (mm yr⁻¹)	1981–1992	12	**+31.50**	0.047	*
	Precip. (mm yr⁻¹)	1993–2025	33	**−3.01**	0.221	**ns**
Kara	Precip. (mm yr⁻¹)	1981–1992	12	**+29.53**	0.115	**ns**
	Precip. (mm yr⁻¹)	1993–2025	33	**−5.64**	0.141	**ns**
Mango	Precip. (mm yr⁻¹)	1981–1992	12	**−12.84**	0.451	**ns**
	Precip. (mm yr⁻¹)	1993–2025	33	**+1.16**	0.609	**ns**
Temperature (°C dec⁻¹)						
Sokodé	Temp. (°C dec⁻¹)	1981–2002	22	**+0.186**	0.032	*
	Temp. (°C dec⁻¹)	2003–2025	23	**+0.216**	0.057	**ns**
Kara	Temp. (°C dec⁻¹)	1981–2002	22	**+0.009**	0.955	**ns**
	Temp. (°C dec⁻¹)	2003–2025	23	**+0.333**	0.003	**
Mango	Temp. (°C dec⁻¹)	1981–2002	22	**+0.308**	0.011	*
	Temp. (°C dec⁻¹)	2003–2025	23	**+0.109**	0.355	**ns**

*Precipitation split year: 1992 (exploratory; most probable Pettitt CP, p = 0.566, not significant). Temperature split year: 2002 (statistically significant Pettitt CP, p < 0.001 at all stations). Significance levels: *** p ≤ 0.001; ** p ≤ 0.01; * p ≤ 0.05; ns = not significant (p > 0.05). Values of p between 0.05 and 0.10 are reported as ns with the exact p-value given.*

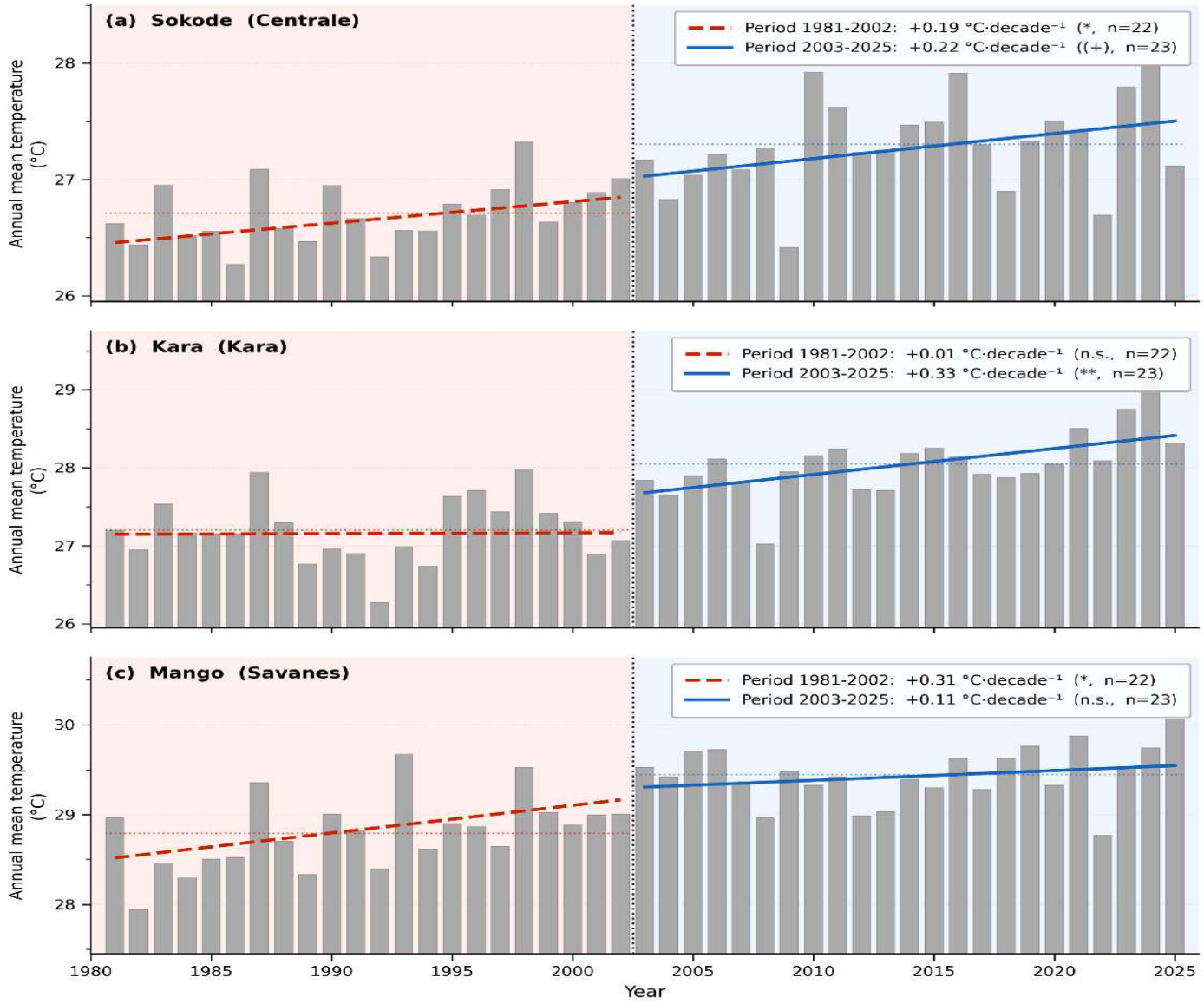


Fig. 7 Sub-period trend analysis for annual mean temperature at Northern Togo stations (1981-2025). Temperature split year: 2002 (Pettitt CP, $p < 0.001$). Orange shaded: pre-warming phase 1981-2002 (n = 22); blue shaded: post-warming phase 2003-2025 (n = 23). Dashed lines: Sen's slope for each sub-period. Significance: ** $p \leq 0.01$; * $p \leq 0.05$; (+) $p \leq 0.10$; ns = not significant.

3.5 Spatial trends in MI, SPI, and SPEI and satellite-based validation

Although the study area has experienced a permanent water deficit throughout the study period (MI <0 in all cases and locations), positive trends in the MI, SPI and SPEI suggest that this deficit has gradually decreased over time, primarily due to increased precipitation in the Sahel since 1990. These two aspects are not contradictory; a region can have a structural water deficit while also experiencing improved vegetation conditions.

The spatial distributions of MK Z statistics and Sen slopes for MI, SPI and, SPEI (Fig. 8) reveal a significantly positive humidification trend concentrated in the Kara region and the southern part of the Central Region. This is consistent with the Sahel's recovery since 1990 (Lebel and Ali 2009; Rauch et al. 2025) and the positive SPEI trends identified across the Sudanese zone by Ogunrinde et al. (2024). Significant negative trends are observed in less than 8% of grid cells for all indices and significance levels. These trends are concentrated in the northeast (Savannah region), which is consistent with convergence towards Saharan conditions. The strong correlation between the CMI, CSPI and CSPEI trends slopes ($\rho s = 0.94\text{-}0.99$, $p < 0.01$; Table 7) confirms that the three indices consistently respond to the same large-scale dynamics.

A pixel-by-pixel analysis of CHIRPS v2.0 (Fig. 9) confirms these results. The annual average rainfall in the region shows positive trends in all three zones: Savanes: +3.17 mm per year ($p = 0.010$); Kara: +2.69 mm per year ($p = 0.047$); and Centrale: +2.81 mm per year, $p = 0.126$). Around 50% of CHIRPS pixels show statistically significant positive trends ($p \leq 0.05$). The positive cumulative trend in the Savanes region (+139 mm over 44 years) equates to approximately 13% of the region's annual average precipitation (1,051 mm per year), which is equivalent to an extra month's worth of water available for crop growth during this period. However, this modest improvement has not yet resulted in a statistically significant change in precipitation. Local negative trends in the Sen slopes series in a small number of pixels in the southern part of the central zone should be interpreted with caution pending confirmation by denser surface observations.

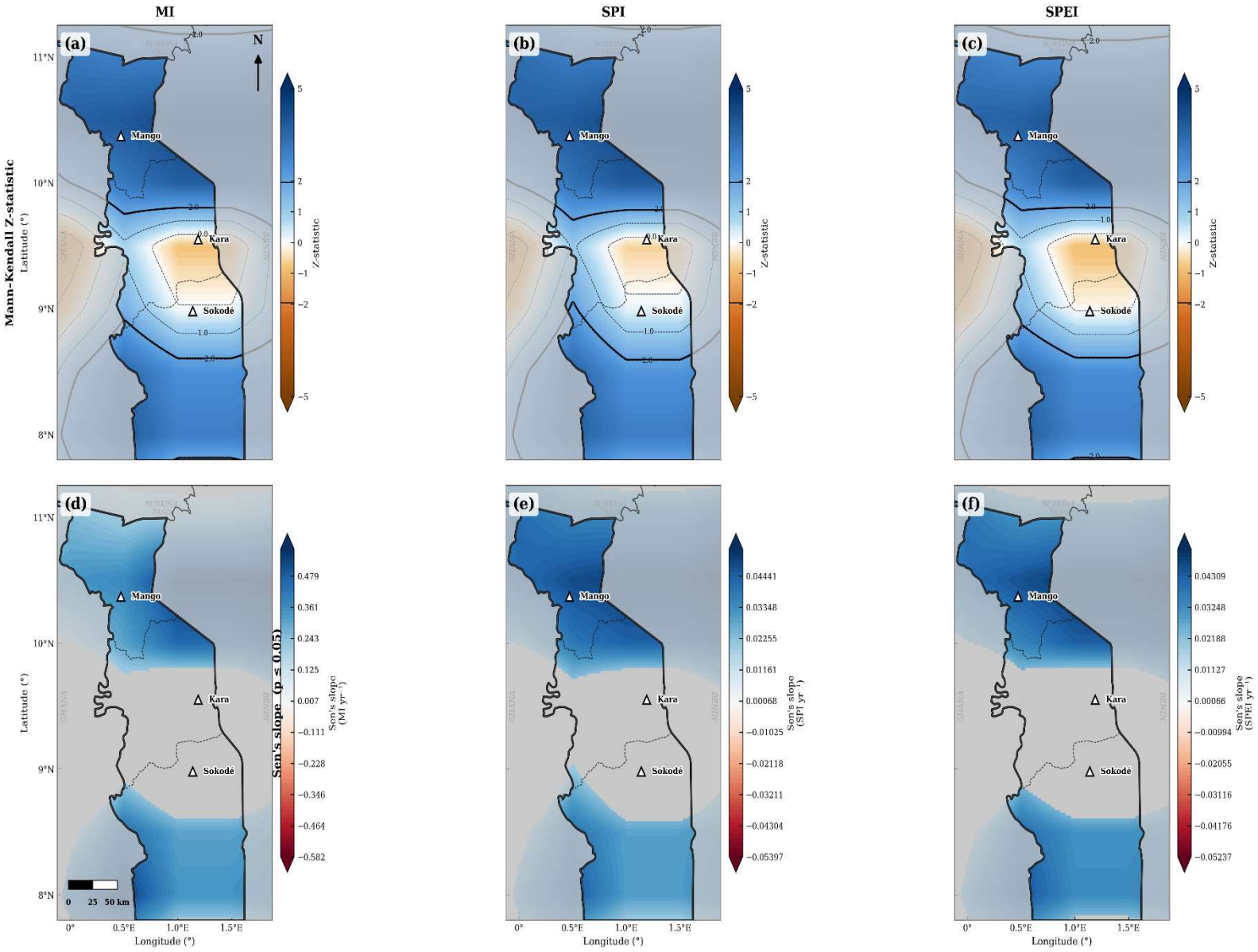
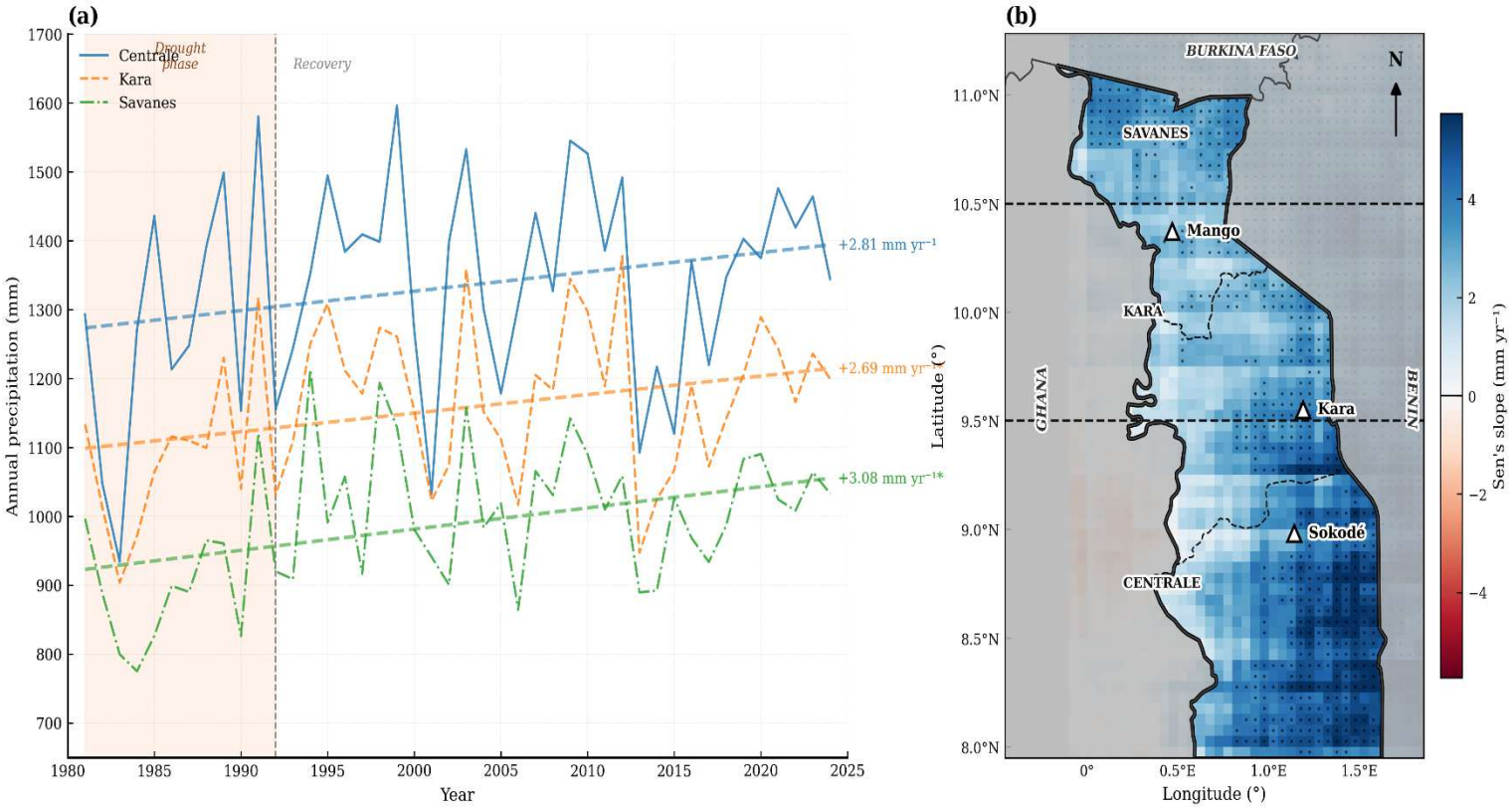


Fig. 8 Spatial distribution of Mann–Kendall trend statistics for annual moisture indices over Northern Togo (1981-2024). **(a-c)** Z-statistic for MI, SPI, and SPEI, respectively; solid contour: $|Z| = 1.96$ ($p = 0.05$). **(d-f)** Sen's slope at grid cells is significant at $p \leq 0.05$; grey = non-significant; blue = wetting trend; red = drying trend. Data: NASA POWER reanalysis (0.5° grid). PET: Hargreaves-Samani (1985); MI: Willmott and Feddema (1992); SPI: McKee *et al.* (1993); SPEI: Vicente-Serrano *et al.* (2010).



476

477 **Fig. 9** CHIRPS v2.0 precipitation trend analysis for Northern Togo (1981-2024, 0.05° resolution).
478 (a) Regional mean annual precipitation for the three agro-ecological zones with Sen's slope
479 annotated; significance: * $p \leq 0.05$, ** $p \leq 0.01$; shaded band: Sahelian drought phase (1981-1992).
480 (b) Pixel-wise Sen's slope (mm yr^{-1}); black dots: significant pixels ($p \leq 0.05$); blue = increasing,
481 red = decreasing precipitation.

482 **3.6 Agricultural and domestic water supply implications**

483 The period from July to September (JAS) accounts for 55 to 65 per cent of annual precipitation
484 and coincides with the main growth period for crops such as sorghum, corn and millet. As can be
485 seen in Figure 10, the JAS SPI-3 and SPEI-3 time series show that SPEI-3 values have been
486 systematically lower than SPI-3 values since 2000. This is attributed to an increase in temperature
487 of between 0.27 and 0.34 °C per decade since 2002. A year with average precipitation (SPI-3 ≈ 0)
488 can be considered moderately arid (SPEI-3 ≤ -1.0) due to high evapotranspiration rates. This
489 differentiation is not evident in a monitoring system based exclusively on precipitation, but it is
490 fundamental for managing the harvest calendar. Gadedjisso-Tossou et al. (2021) conducted a

multiple regression analysis using historical climate and crop productivity data from stations in northern Togo (Kara, Mango, Niamtougou, and Dapaong). They demonstrated that increased maximum temperatures significantly reduce the productivity of corn, sorghum and millet due to their effect on evapotranspiration. Based on this documented sensitivity, SPI-3 values below -1.5 in Mango and Kara in 2025 are consistent with water deficits during the growth period. This results in yield losses of over 25-35% in cereals planted in humid areas (Gadedjisso-Tossou et al. 2021; Sultan et al. 2013). Severe droughts during the rainy season (JAS) in 2024-2025 are consistent with food security assessments by FEWS NET and the FAO in northern Togo during the 2024-2025 harvest period, thus validating local drought indices.

The progressive divergence between the SPI and SPEI indices since 2003 indicates a decrease in aquifer recharge efficiency, even during periods of average precipitation. This increases the structural vulnerability of the savannah's water system.
Therefore, investments in the artificial recharge of aquifers, rainwater harvesting and community groundwater monitoring are urgent.

In terms of drinking water supply, northern Togo relies primarily on shallow wells (less than 15 metres deep) and small seasonal rivers, particularly in the Mango, Dapaong and Cinkassé regions. In the semi-arid regions of West Africa, shallow and unconfined aquifers are recharged episodically, mainly by intense seasonal rainfall. Long droughts can cause aquifer levels to drop, with the effects lasting for years (Taylor et al. 2013). MacDonald et al. (2021) estimated that semi-arid regions in Africa experience an annual recharge rate of around 60 mm (ranging from 30 to 140 mm), equivalent to 5-6% of the annual precipitation In northern Togo, where the annual precipitation average is 1,050-1,270 mm, this equates to an annual aquifer recharge of 53-76 mm under current conditions. However, this amount is highly sensitive to interannual variability in precipitation and is at risk of being compromised by the increase in temperatures observed since 2002. This increase in temperatures increases evapotranspiration and reduces the amount of precipitation available for aquifer recharge (Granata and Di Nunno 2025). The progressive divergence in values between the SPI and SPEI indices since 2003 indicates a decrease in effective groundwater recharge, even during years of moderate precipitation. This is because growing evapotranspiration retains more rainwater, preventing it from infiltrating shallow aquifers. This

mechanism exacerbates the region's structural vulnerability to water supply issues, which became dramatically apparent during the 2025 hydrological year. The Kozah dam, which is the main source of water for the Kozah, Doufelgou and Binah provinces in the Kara region, reached a historically low level by the end of the 2025 rainy season. The water level dropped from 16 metres in 2024 to less than 8 metres in October 2025, reaching 5.3 metres in December of the same year (Ministry of Environment of Togo, 2025). This 50% decrease reduced daily drinking water production by around 40%, from 11,000 m^3 to 4,500 m^3 per day. This was well below the estimated daily demand of 20,000 m^3 for the Kara urban region. The crisis worsened due to evaporation caused by high temperatures and absorption by alternative water sources. This prompted the Togolese government to take emergency measures, including rehabilitating 50 existing wells and constructing 14 new ones, as well as enacting national parliamentary intervention on 31 December 2025 (Togolese National Assembly, 2025). Therefore, urgent investment is needed in the artificial recharge of aquifers, rainwater harvesting and community monitoring of groundwater to reduce the Kara region's structural dependence on a single surface infrastructure that is becoming increasingly vulnerable to climate change.



Fig. 10 July-August-September (JAS) agricultural growing-season drought indices for Northern Togo (1981-2025). Bars: SPI-3 (blue = wet, red = dry); line: SPEI-3 (orange). Dashed lines: moderate (-1.0) and severe (-1.5) drought thresholds. Shaded band: Sahelian drought phase (1981-1992). Note the systematic SPEI-3 downward shift relative to SPI-3 post-2000, driven by warming-amplified evapotranspiration demand.

4 Conclusions

This study analyses annual, seasonal and monthly trends in precipitation, drought characteristics and water deficits in northern Togo's three agroecological zones from 1981 to 2025. No significant precipitation trends were detected at any station ($p > 0.40$ for all), as confirmed by the Hamed-Rao and standard Mann-Kendall tests. The most severe drought episodes were recorded in Sokodé in 1982 (Standardized Precipitation Index, SPI = -2.02), at Mango in 2025 (SPI = -2.16) and at Kara in 2025 (SPI = -1.94), consistent with FEWS NET and FAO food security assessments for the 2024-2025 lean season in northern Togo.

Throughout the entire study period, all NASA-POWER grid cells and the three synoptic stations recorded exclusively negative Moisture Index (MI) values, confirming a permanent water-deficit across the entire region (Fig. 6 and 7, and Tables 6 and 7). MI values varied between -20 in the southern central plains to -60 in the northeastern Savanes region, reflecting the aridity gradient from north to south confirmed by Spearman rank correlations. The dominant spatial controls on moisture availability were geographic latitude ($\rho s = -0.865$, $p < 0.01$) and potential evapotranspiration (PET) ($\rho s = -0.929$, $p < 0.01$), while precipitation played a secondary but significant role ($\rho s = +0.757$, $p < 0.01$). MI values below -20, the semi-arid threshold, were recorded across all years and stations, indicating that subsistence agriculture operates permanently below the hydric safety limit. The maximum MI value recorded in Kara (-2.9) indicates that the Short Grass Savanna zone can approach hydric equilibrium during exceptionally abundant monsoon years, consistent with the orographic influence of the Atacora mountain chain.

This study has revealed that the hydrological dynamics in northern Togo are more complex than previously characterised. While precipitation has remained without a significant trend, the water balance deficit has widened substantially since 2003 due to warming-driven evapotranspiration demand, intensifying agricultural drought risk in a manner invisible to precipitation-only monitoring systems. Given the documented sensitivity of cereal crops to growing-season water deficits, SPI-3 values below -1.5 at Mango and Kara in 2025 are consistent with rain-fed cereal yield losses exceeding 25-35%, directly threatening SDG 2 (Zero Hunger; specifically Target 2.4 on sustainable food production systems and climate-resilient agricultural practices).

Reduced surface water and groundwater recharge further endangers the region's domestic water supply, with consequences extending well beyond the agricultural sector. The Kozah reservoir, the primary source of drinking water for the Kozah, Doufelgou and Binah prefectures in the Kara region since its operation began in 1979, reached a historically unprecedent low level at the end of the 2025 rainy season, falling from 16 m in 2024 to 5.30 m by December 2025. This 50% decline reduced daily drinking water production by 40%, necessitating emergency governmental intervention that was approved by parliament on 31 December 2025. This crisis is directly consistent with the abrupt temperature step-change documented around 2001-2003 in this study: rising evapotranspiration demand at Kara (+0.34 °C per decade, $p < 0.001$) reduces the fraction of seasonal rainfall available for surface water storage and aquifer recharge, amplifying drought impacts beyond what precipitation levels suggest. This threatens the achievement of SDG 6 (clean water and sanitation; Target 6.4 on water-use efficiency and freshwater availability). The pace of warming since 2002 further underscores the urgent need for local adaptation measures consistent with SDG 13 (climate action; Target 13.1 on resilience and adaptive capacity to climate hazards). It is therefore recommended that agricultural extension services promote drought-tolerant and early-maturing crop varieties, and advise farmers to adjust planting calendars to account for the increasing concentration of rainfall in the late growing season. Investment should be directed toward supplemental irrigation infrastructure, managed aquifer recharge, diversification of water sources beyond single surface reservoirs, and community-scale groundwater monitoring in the Kara, Mango and Dapaong sub-regions.

In the context of the 2030 Agenda, the development of an integrated drought early-warning system calibrated to the three agro-ecological zones of northern Togo represents a critical step toward climate-resilient development. During the July-September growing season, the system should monitor SPEI-3 values and trigger alerts when they fall below -1.0 (the moderate drought threshold). Operational management should be led by the Direction Générale de la Météorologie Nationale du Togo (DGMN) in collaboration with national agricultural advisory services. Future research should focus on hydrological drought propagation analysis, integration of CMIP6 downscaled projections, and development of a spatially distributed drought monitoring system for the region.

Acknowledgements The author expresses gratitude to Direction Générale de la Météorologie Nationale du Togo (DGMN) for assisting this research with datasets.

Author contribution This work is part of the doctoral (PhD) thesis of Malaguièhèwa Grâce Pekeyi, conducted under the supervision of Prof. Appollonia Aimiosino Okhimamhe, Prof. Tayo Iyanda Yahaya, and Dr. Isaiah Sule. Malaguièhèwa Grâce Pekeyi was responsible for Conceptualization, Data curation, Formal analysis, Methodology, Visualization, Software, and Writing of the original draft. Supervision was provided by Appollonia Aimiosino Okhimamhe, Tayo Iyanda Yahaya, and Isaiah Sule.
I declare that all authors reviewed the manuscript. All authors read and approved the final manuscript.

Funding This research was conducted with the support of The Homegrown Clean Energy (HCE) Solutions through the Entrepreneurship Centre of the Federal University of Technology Minna (FUTMINNA), Nigeria.

Data availability NASA POWER monthly climate data are freely available through the NASA POWER Data Access Viewer at https://power.larc.nasa.gov/.
CHIRPS v2.0 monthly precipitation data are available from the Climate Hazards Group at https://www.chc.ucsb.edu/data/chirps.

The Copernicus GLO-30 DEM is publicly available at

https://dataspace.copernicus.eu/explore-data/data-collections/copernicus-contributing-missions/collections-description/COP-DEM.
Station precipitation and temperature records for 1981-2025 were provided by the Direction Générale de la Météorologie Nationale du Togo (DGMN) under a data-sharing agreement; access requests should be directed to the DGMN (B.P. 64, Lomé, Togo).

Declarations

Consent for publication Not applicable.

Ethics approval and consent to participate Not applicable.

Competing interests The authors declare no competing interests.

Clinical Trial Registration Not applicable

References

Ababio, P.K., Antwi-Agyei, P. and Azumah, S.B. (2024) West Africa's Drought Dynamics: An Investigation of SPI and SPEI indices (1979-2021). *Int. J. Phys. Res. Appl.* **7**(1), 1–12. doi:10.29328/journal.ijpra.1001093

Alexandersson, H. (1986) A homogeneity test applied to precipitation data. doi:10.1002/joc.3370060607

Ali, E. (2021) Farm Households' Adoption of Climate-smart Practices in Subsistence Agriculture: Evidence from Northern Togo. *Environ. Manage.* **67**(5), 949–962. doi:10.1007/s00267-021-01436-3

Allan, R., Pereira, L. & Smith, M. (1998) *Crop evapotranspiration-Guidelines for computing crop water requirements-FAO Irrigation and drainage paper 56*, Vol. 56.

Assemblée nationale togolaise (2025) Parliamentary question of current affairs: the government responds to drinking water supply difficulties in certain regions of the country. Plenary session of 31 December 2025. Lomé: National Assembly of Togo. https://assemblee-nationale.tg/question-dactualite-le-gouvernement-repond-aux-difficultes-dapprovisionnement-en-eau-potable-dans-certaines-regions-du-pays/

Barbé, L. L., Lebel, T. & Tapsoba, D. (2002) Rainfall Variability in West Africa during the Years 1950–90. Retrieved from https://journals.ametsoc.org/view/journals/clim/15/2/1520-0442_2002_015_0187_rviwad_2.0.co_2.xml

Beguería, S., Vicente-Serrano, S. M., Reig, F. & Latorre, B. (2014) Standardized precipitation evapotranspiration index (SPEI) revisited: parameter fitting, evapotranspiration models, tools, datasets and drought monitoring. *Int. J. Climatol.* **34**(10), 3001–3023. doi:10.1002/joc.3887

Biasutti, M. (2019) Rainfall trends in the African Sahel: Characteristics, processes, and causes. *WIREs Clim. Change* **10**(4), e591. doi:10.1002/wcc.591

Bodjrènou, R., Sintondji, L. O., Sambieni, S. K., Tidjani, N., Koyo, P., Avossè, A. & Comandan, F. (2025) Analysis of current and future climate variability and drought recurrence in Benin, West Africa. *J. Water Clim. Change* **16**(7), 2297–2316. doi:10.2166/wcc.2025.842

Buishand, T. A. (1982) Some methods for testing the homogeneity of rainfall records. *J. Hydrol.* **58**(1), 11–27. doi:10.1016/0022-1694(82)90066-X

Calvin, K., Dasgupta, D., Krinner, G., Mukherji, A., Thorne, P. W., Trisos, C., Romero, J., et al. (2023) IPCC, 2023: Climate Change 2023: Synthesis Report. Contribution of Working Groups I, II and III to the Sixth Assessment Report of the Intergovernmental Panel on Climate Change [Core Writing Team, H. Lee and J. Romero (eds.)]. IPCC, Geneva, Switzerland. Intergovernmental Panel on Climate Change. doi:10.59327/ipcc/ar6-9789291691647

Cosgrove, W., Rijsberman, F. & Water, C. (2000) *World Water Vision: Making Water Everybody's Business*. doi:10.4324/9781315071763

Djaman, K. (2017) Spatial and Temporal Variation in Precipitation in Togo. *Int. J. Hydrol.* **1**(4). doi:10.15406/ijh.2017.01.00019

Djaman, K. & Ganyo, K. (2015) Trend analysis in reference evapotranspiration and aridity index in the context of climate change in Togo. *J. Water Clim. Change*. doi:10.2166/wcc.2015.111

Droogers, P. & Allen, R. G. (2002) Estimating Reference Evapotranspiration Under Inaccurate Data Conditions. *Irrig. Drain. Syst.* **16**(1), 33–45. doi:10.1023/A:1015508322413

689 Funk, C., Peterson, P., Landsfeld, M., Pedreros, D., Verdin, J., Shukla, S., Husak, G., et al. (2015)
690 The climate hazards infrared precipitation with stations—a new environmental record for
691 monitoring extremes. *Sci. Data* **2**(1), 150066. Nature Publishing Group.
692 doi:10.1038/sdata.2015.66
693 Gadedjisso-Tossou, A., Adjegan, K. I. & Kablan, A. K. M. (2021) Rainfall and Temperature Trend
694 Analysis by Mann–Kendall Test and Significance for Rainfed Cereal Yields in Northern
695 Togo. *Sci* **3**(1), 17. Multidisciplinary Digital Publishing Institute. doi:10.3390/sci3010017
696 Gocic, M. & Trajkovic, S. (2013) Analysis of changes in meteorological variables using Mann-
697 Kendall and Sen's slope estimator statistical tests in Serbia. *Glob. Planet. Change* **100**,
698 172–182. doi:10.1016/j.gloplacha.2012.10.014
699 Granata, F. & Di Nunno, F. (2025) Rising threats to groundwater recharge: Adaptive strategies for
700 the Sahel under climate change. *Groundw. Sustain. Dev.* **30**, 101468.
701 doi:10.1016/j.gsd.2025.101468
702 Hamed, K. H. & Ramachandra Rao, A. (1998) A modified Mann-Kendall trend test for
703 autocorrelated data. *J. Hydrol.* **204**(1), 182–196. doi:10.1016/S0022-1694(97)00125-X
704 Hargreaves, G. & Samani, Z. (1985) Reference Crop Evapotranspiration From Temperature. *Appl.*
705 *Eng. Agric.* **1**. doi:10.13031/2013.26773
706 Hersbach, H., Bell, B., Berrisford, P., Hirahara, S., Horányi, A., Muñoz-Sabater, J., Nicolas, J., et
707 al. (2020) The ERA5 global reanalysis. *Q. J. R. Meteorol. Soc.* **146**(730), 1999–2049.
708 doi:10.1002/qj.3803
709 Hussain, M. M. & Mahmud, I. (2019) pyMannKendall: a python package for non parametric Mann
710 Kendall family of trend tests. *J. Open Source Softw.* **4**(39), 1556. doi:10.21105/joss.01556
711 Intergovernmental Panel on Climate Change (IPCC) (2021) *Climate Change 2021 – The Physical*
712 *Science Basis: Working Group I Contribution to the Sixth Assessment Report of the*
713 *Intergovernmental Panel on Climate Change*. Cambridge: Cambridge University Press.
714 doi:10.1017/9781009157896
715 Kohler, M. A. (1949) On the Use of Double-Mass Analysis for Testing the Consistency of
716 Meteorological Records and for Making Required Adjustments. doi:10.1175/1520-0477-
717 30.5.188
718 Kongo, V. O. & Arreyndip, N. A. (2025) The 2023 drought in West Africa and associated
719 vulnerability to food insecurity. *Sci. Rep.* **15**(1), 34959. Nature Publishing Group.
720 doi:10.1038/s41598-025-18940-9
721 Koudahe, K., Kayode, A. J., Samson, A. O., Adebola, A. A. & Djaman, K. (2017) Trend Analysis
722 in Standardized Precipitation Index and Standardized Anomaly Index in the Context of
723 Climate Change in Southern Togo. *Atmospheric Clim. Sci.* **07**(04), 401–423.
724 doi:10.4236/acs.2017.74030
725 Lebel, T. & Ali, A. (2009) Recent trends in the Central and Western Sahel rainfall regime (1990-
726 2007). *J. Hydrol.* **375**(1–2). Journal of Hydrology. doi:10.1016/j.jhydrol.2008.11.030
727 MacDonald, A. M., Lark, R. M., Taylor, R. G., Abiye, T., Fallas, H. C., Favreau, G., Goni, I. B.,
728 et al. (2021) Mapping groundwater recharge in Africa from ground observations and
729 implications for water security. *Environ. Res. Lett.* **16**(3), 034012. IOP Publishing.
730 doi:10.1088/1748-9326/abd661
731 Mao, D. & Cherkauer, K. A. (2009) Impacts of land-use change on hydrologic responses in the
732 Great Lakes region. *J. Hydrol.* **374**(1), 71–82. doi:10.1016/j.jhydrol.2009.06.016

Mccabe, G. & Wolock, D. (2007) Sensitivity of Irrigation Demand in a Humid-Temperate Region to Hypothetical Climatic Change. *JAWRA J. Am. Water Resour. Assoc.* **28**, 535–543. doi:10.1111/j.1752-1688.1992.tb03175.x

McKee, T. B., Doesken, N. J. & Kleist, J. (1993) THE RELATIONSHIP OF DROUGHT FREQUENCY AND DURATION TO TIME SCALES.

Mishra, A. K. & Singh, V. P. (2010) A review of drought concepts. *J. Hydrol.* **391**(1), 202–216. doi:10.1016/j.jhydrol.2010.07.012

Ministère de l'Aménagement du Territoire, de l'Urbanisme et de l'Habitat du Togo (2025) Early drought in the Kara region: government response. Official communiqué, December 2025. Lomé: Republic of Togo. https://urbanisme.gouv.tg/kara-le-gouvernement-accelere-les-travaux-dadduction-deau-potable/

Nicholson, S. E. (2013) The West African Sahel: A Review of Recent Studies on the Rainfall Regime and Its Interannual Variability. *Int. Sch. Res. Not.* **2013**(1), 453521. doi:10.1155/2013/453521

Nkrumah, F., Klutse, N. A. B., Adukpo, D. C., Owusu, K., Quagraine, K. A., Owusu, A. & Gutowski, W. (2014) Rainfall Variability over Ghana: Model versus Rain Gauge Observation. *Int. J. Geosci.* **5**(7), 673–683. Scientific Research Publishing. doi:10.4236/ijg.2014.57060

Ogunrinde, A. T., Oguntunde, P. G., Akinwumiju, A. S. & Fasinmirin, J. T. (2019) Analysis of recent changes in rainfall and drought indices in Nigeria, 1981–2015. *Hydrol. Sci. J.* **64**(14), 1755–1768. doi:10.1080/02626667.2019.1673396

Ogunrinde, Akinwale T., Adigun, P., Xian, X., Yu, H., Koji, D., Adebiyi, A. & Sabo, A. A. (2024) Multi-scale drought variability over West Africa and the associated large-scale circulation patterns. *Geomat. Nat. Hazards Risk* **15**(1), 2409199. Taylor & Francis. doi:10.1080/19475705.2024.2409199

Panthou, G., Lebel, T., Vischel, T., Quantin, G., Sane, Y., Ba, A., Ndiaye, O., et al. (2018) Rainfall intensification in tropical semi-arid regions: the Sahelian case. *Environ. Res. Lett.* **13**(6), 064013. IOP Publishing. doi:10.1088/1748-9326/aac334

Pettitt, A. N. (1979) A Non-Parametric Approach to the Change-Point Problem. *Appl. Stat.* **28**(2), 126. JSTOR. doi:10.2307/2346729

Rauch, M., Bliefernicht, J., Maranan, M., Fink, A. H. & Kunstmann, H. (2025) Interannual Rainfall Variability in West Africa: Reconstruction Based on Atmospheric Circulation Patterns. *Int. J. Climatol.* **45**(14), e70088. doi:10.1002/joc.70088

Sen, P. K. (1968) Estimates of the Regression Coefficient Based on Kendall's Tau. *J. Am. Stat. Assoc.* **63**(324), 1379–1389. Taylor & Francis. doi:10.1080/01621459.1968.10480934

Spinoni, J., Barbosa, P., De Jager, A., McCormick, N., Naumann, G., Vogt, J. V., Magni, D., et al. (2019) A new global database of meteorological drought events from 1951 to 2016. *J. Hydrol. Reg. Stud.* **22**, 100593. doi:10.1016/j.ejrh.2019.100593

Storch, H. von. (1995) Misuses of Statistical Analysis in Climate Research. In: *Analysis of Climate Variability: Applications of Statistical Techniques* (H. von Storch & A. Navarra, eds), 11–26. Berlin, Heidelberg: Springer. doi:10.1007/978-3-662-03167-4_2

Sultan, B., Roudier, P., Quirion, P., Alhassane, A., Muller, B., Dingkuhn, M., Ciais, P., et al. (2013) Assessing climate change impacts on sorghum and millet yields in the Sudanian and Sahelian savannas of West Africa. *Environ. Res. Lett.* **8**(1), 014040. IOP Publishing. doi:10.1088/1748-9326/8/1/014040

Sylla, M. B., Giorgi, F., Coppola, E. & Mariotti, L. (2013) Uncertainties in daily rainfall over Africa: assessment of gridded observation products and evaluation of a regional climate model simulation. *Int. J. Climatol.* **33**(7), 1805–1817. doi:10.1002/joc.3551

Taylor, R. G., Scanlon, B., Döll, P., Rodell, M., Beek, R. van, Wada, Y., Longuevergne, L., et al. (2013) Ground water and climate change. *Nat. Clim. Change* **3**(4), 322–329. Nature Publishing Group. doi:10.1038/nclimate1744

Tazen, F., Diarra, A., Kabore, R. F. W., Ibrahim, B., Bologo/Traoré, M., Traoré, K. & Karambiri, H. (2019) Trends in flood events and their relationship to extreme rainfall in an urban area of Sahelian West Africa: The case study of Ouagadougou, Burkina Faso. *J. Flood Risk Manag.* **12**(S1), e12507. doi:10.1111/jfr3.12507

Tefera, M. L., Giovanna Seddaiu, Alberto Carletti & Awada, H. (2024) Rainfall variability and drought in West Africa: challenges and implications for rainfed agriculture. *Theor. Appl. Climatol.* **156**(1), 41. doi.org/10.1007/s00704-024-05251-8

Vicente-Serrano, S. M., Beguería, S. & López-Moreno, J. I. (2010) A Multiscalar Drought Index Sensitive to Global Warming: The Standardized Precipitation Evapotranspiration Index. doi:10.1175/2009JCLI2909.1

Wang, X. & Liu, L. (2023) The Impacts of Climate Change on the Hydrological Cycle and Water Resource Management. *Water* **15**(13), 2342. MDPI AG. doi:10.3390/w15132342

Wilhite, D. A. & Glantz, M. H. (1985) Understanding: the Drought Phenomenon: The Role of Definitions. *Water Int.* **10**(3), 111–120. Routledge. doi:10.1080/02508068508686328

Willmott, C. J. & Feddema, J. J. (1992) A More Rational Climatic Moisture Index*. *Prof. Geogr.* **44**(1), 84–88. Routledge. doi:10.1111/j.0033-0124.1992.00084.x

Yaméogo, J. (2024) Changes in the seasonal cycles of extreme temperatures in the Sudano-Sahelian domain in West Africa: a case study from Burkina Faso. *Meteorol. Hydrol. Water Manag.* **12**(2). doi:10.26491/mhwm/194451

Yao, K. M. A., Kola, E., Morenikeji, W. & Filho, W. L. (2023) Time Series Analysis of Temperature and Rainfall in the Savannah Region in Togo, West Africa. *Water* **15**(9), 1656. Multidisciplinary Digital Publishing Institute. doi:10.3390/w15091656

Zhang, T., Stackhouse Jr, P., Chandler, W., Hoell, J., Westberg, D. & Whitlock, C. (2010) A GLOBAL ASSESSMENT OF SOLAR ENERGY RESOURCES: NASA's Prediction of Worldwide Energy Resources (POWER) Project. *AGU Fall Meet. Abstr.*